



Short communication

Morphologically controlled Co_3O_4 nanodisks as practical bi-functional catalyst for rechargeable zinc–air battery applications



Dong Un Lee, Jordan Scott, Hey Woong Park, Salah Abureden, Ja-Yeon Choi, Zhongwei Chen*

Department of Chemical Engineering, Waterloo Institute for Nanotechnology, Waterloo Institute for Sustainable Energy, University of Waterloo, Waterloo, ON, Canada

ARTICLE INFO

Article history:

Received 20 February 2014

Received in revised form 13 March 2014

Accepted 20 March 2014

Available online 29 March 2014

Keywords:

Cobalt oxide

Bi-functional catalyst

Oxygen reduction reaction

Oxygen evolution reaction

Rechargeable

Zinc–air battery

ABSTRACT

The morphological control of Co_3O_4 by polyvinylpyrrolidone during precipitation reaction has resulted in the formation of two-dimensional nanodisks with surface porosity. As a bi-functional catalyst, Co_3O_4 nanodisks are active towards both the oxygen reduction and evolution reactions. The electrocatalytic activity is evaluated by preparing air electrodes for rechargeable zinc–air batteries utilizing ambient air to emphasize practicality. The galvanodynamic charge and discharge behaviors are far superior than Co_3O_4 nanoparticle counterparts particularly at high applied current densities. Electrochemical impedance spectroscopy reveals that Co_3O_4 nanodisk electrode results in significantly less internal, solid-electrolyte interface, and charge transfer resistances which lead to highly efficient electrochemical reactions. Superior rechargeability has also been confirmed where virtually no voltage drops are observed over 60 pulse cycles. The practicality of Co_3O_4 nanodisks is highlighted by demonstrating comparable discharge voltages and greatly outperforming charge voltages with excellent electrochemical stability than commercial Pt/C catalyst.

© 2014 Elsevier B.V. All rights reserved.

1. Introduction

With rising price of fossil fuels and its limited nature, the need for advanced energy conversion and storage devices has never been higher. Metal–air batteries, such as zinc–air and lithium–air batteries, are promising candidates for the next generation energy storage device, which have extremely high theoretical specific energy density for applications such as electric vehicles [1–4]. In addition, metal–air batteries utilize oxygen in the air as the source of fuel, which eliminate on-board fuel reservoir and the use of expensive intercalation materials to generate energy [1]. In particular, zinc–air batteries are interesting and are being highly investigated for their cost competitiveness, environment benignity, and low operation risks [5,6].

For rechargeable zinc–air batteries, the two primary electrochemical reactions required are oxygen reduction reaction (ORR) and oxygen evolution reaction (OER), which correspond to the discharge and charge processes, respectively. However, the intrinsic kinetics of these reactions are sluggish, hence electrocatalysts are used to lower the activation energy to progress them at practical rates [7]. Bi-functional catalysts are extremely beneficial as they are capable of catalyzing both ORR and OER on a single electrode, greatly simplifying the battery

architecture and cost of the battery [8,9]. The most effective catalysts currently available are those based on noble metals, such as platinum and iridium [10,11], however the high costs and electrochemical instability limit their use in zinc–air batteries and hamper wide commercialization. Having said this, non-precious transition metal oxides such as cobalt based spinels are being actively investigated to develop cost competitive, stable, and efficient bi-functional catalyst [7,8,12]. Herein, we introduce two-dimensional nanodisk morphology of cobalt oxide (Co_3O_4) with surface porosity as highly efficient and stable bi-functional electrode material for rechargeable zinc–air battery applications.

2. Materials and methods

2.1. Preparation of Co_3O_4 nanodisks

In a typical synthesis, a solution of 10 mL mixture of double deionized (DDI) water and ethanol in a 1:1 volume ratio containing 1.65 g of 24,000 molecular weight polyvinylpyrrolidone (PVP) and 1.252 g of $\text{Co}(\text{NO}_3)_2 \cdot 6\text{H}_2\text{O}$ is dissolved by magnetic stirring and bubbled with N_2 for 30 min. Then, 0.213 mL of 1.0 M NaOH solution is added drop-wise at a rate of 0.56 mL min^{-1} resulting in color change of the solution from pink to dark blue as the precipitation reaction proceeds. The mixture is transferred to a sealed Teflon-lined autoclave and heated at $120 \text{ }^\circ\text{C}$ for 6 h. The resulting precipitate is centrifuged three times with DDI water and another three times with acetone at 5000 rpm then freeze-dried for 24 h. Finally, the obtained black powder is calcined in air at $300 \text{ }^\circ\text{C}$ for 3 h to obtain Co_3O_4 nanodisks.

* Corresponding author at: 200 University Ave. West, Waterloo, ON N2L 3G1, Canada. Tel.: +1 519 888 4567x38664.

E-mail address: zhwchen@uwaterloo.ca (Z. Chen).

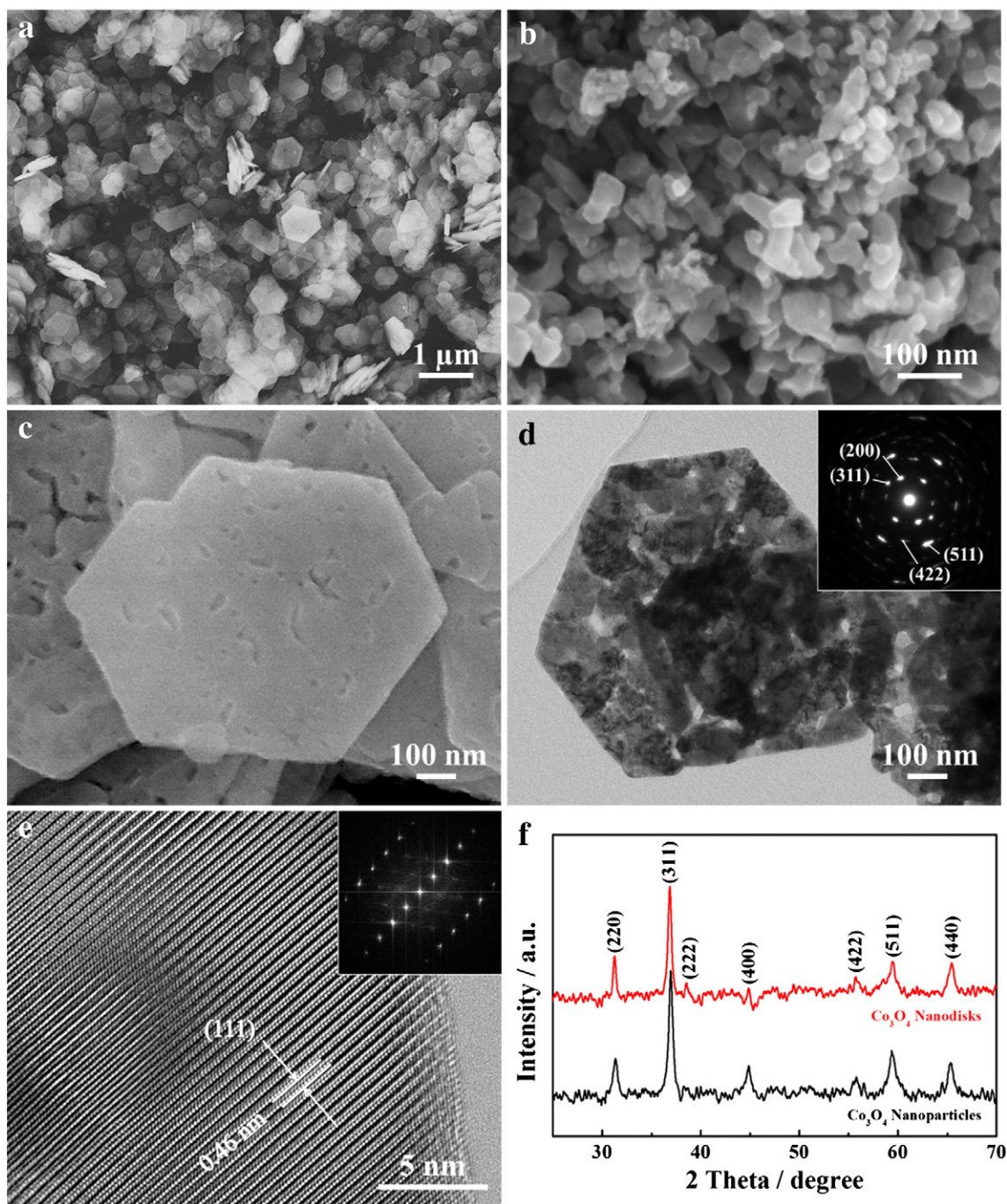


Fig. 1. SEM images of Co_3O_4 (a) nanodisks, (b) nanoparticles, and (c) surface morphology of Co_3O_4 nanodisks. (d) TEM image of Co_3O_4 nanodisks. Inset: SAED pattern. (e) HR-TEM of (111) crystal plane of Co_3O_4 nanodisk. Inset: FFT pattern. (f) XRD patterns of Co_3O_4 nanodisks (red) and nanoparticles (black).

2.2. Materials characterization

Scanning electron microscopy (SEM) (Leo FESEM 1530) and transmission electron microscopy (TEM) (Phillips CM300) are conducted to reveal the morphology and surface features, and high resolution TEM (HR-TEM), fast Fourier transform (FFT) pattern, and selected area electron diffraction (SAED) patterns are used to reveal the crystallinity. X-ray diffraction (XRD) (Bruker AXS D8 Advance) is utilized to confirm the spinel crystal structure of Co_3O_4 nanodisks and nanoparticles.

2.3. Single-cell practical zinc-air battery fabrication

The single-cell catalytic activity is tested by fabricating a home-made zinc-air battery and a multichannel potentiostat (Princeton Applied Research, VersaSTAT MC). For the anode and cathode of the battery, a polished zinc plate (Zinc Sheet EN 988, OnlineMetals) and a catalyst-deposited gas diffusion layer (GDL) (SGL Carbon 10 BB, Ion Power Inc.) are used, respectively. The GDL is prepared by spray-coating a catalyst ink consisting of 10 mg of Co_3O_4 nanodisks and 67 μL of 5 wt.% Nafion (LIQUion™ solution, Ion Power Inc.) dispersed in 1.0 mL

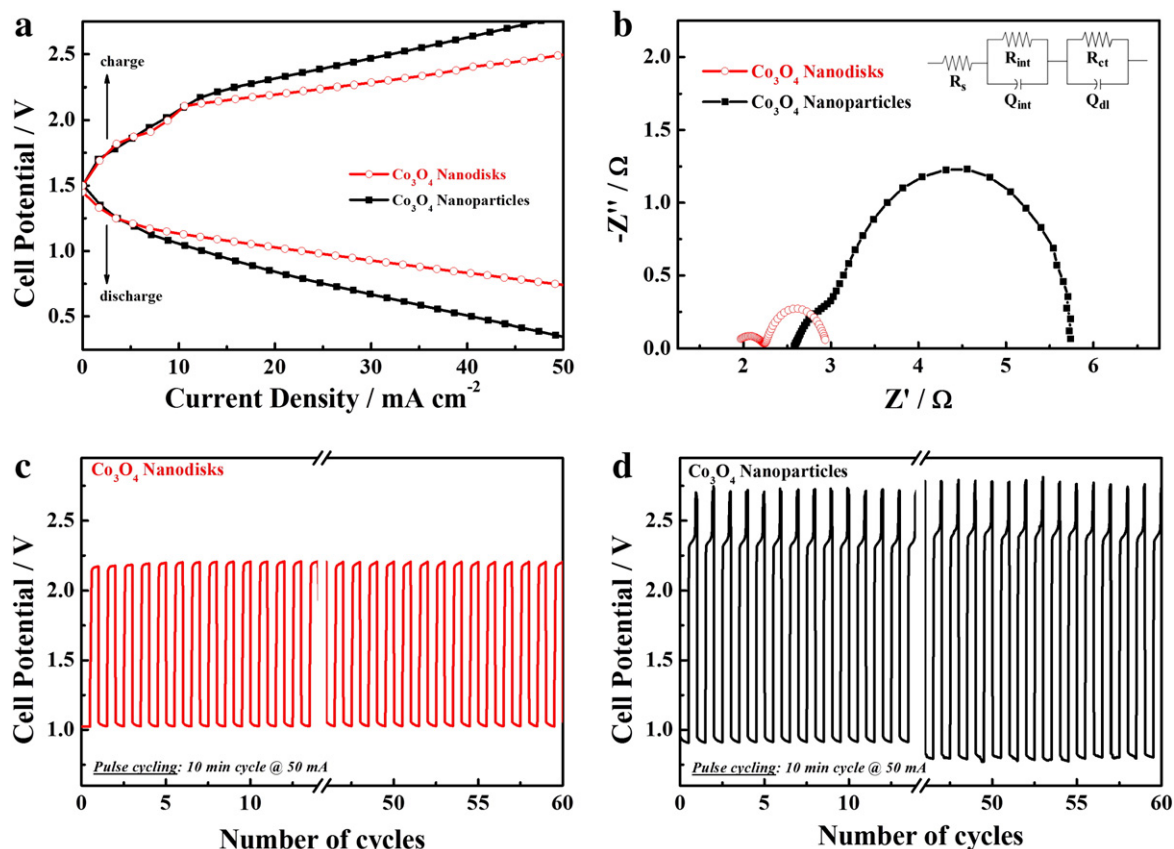


Fig. 2. (a) Galvanodynamic charge/discharge profiles, (b) Nyquist plots (inset: equivalent circuit), and (c, d) galvanostatic pulse cyclings of Co_3O_4 nanodisks (red), and Co_3O_4 nanoparticles (black).

of isopropyl alcohol. Similarly, Co_3O_4 nanoparticle (Sigma-Aldrich) is spray-coated on a GDL with the same loading as a comparison. After spraying, the electrode is dried in an oven at 60°C for 1 h. All electrodes are prepared to achieve a loading of ca. 1.5 mg cm^{-2} with catalytically active surface area of 2.834 cm^2 . The gap between the cathode and anode is 1.0 cm. For the electrolyte and separator, 6.0 M KOH and micro-porous membrane (Celgard 5550) are used, respectively.

2.4. Rechargeable zinc–air battery performance testing

The battery charge and discharge voltages are measured by the galvanodynamic method scaling the current from 0 to 200 mA at a rate of 5 mA s^{-1} . The charge–discharge pulse cycling is tested by the recurrent galvanic pulse method using an applied current of 50 mA with each cycle consisting of 5 min discharge followed by 5 min charge. Electrochemical impedance spectroscopy (EIS) is conducted by operating the battery at constant cell potential of 0.8 V and alternating current (AC) amplitude of 20 mV with its frequency ranging from 100 kHz to 0.1 Hz.

Table 1

Equivalent circuit element values of Co_3O_4 nanodisk and nanoparticle electrodes in a single-cell zinc–air battery.

Elements	R_s	R_{int}	R_{ct}	Q_{int}	Q_{dl}
Nanodisks	1.88	0.384	0.698	0.00514	0.197
Nanoparticles	3.66	0.861	2.97	0.00312	0.00165

3. Results and discussion

The Co_3O_4 catalyst consists of two-dimensional nanodisk structures with relatively characteristic hexagonal geometry having an average diameter and thickness of 500–600 and 20–40 nm, respectively (Fig. 1a). The nanodisk morphology is created by confining the growth only into two dimensions using PVP as the capping agent which specifically adsorbs onto certain crystal planes to inhibit their growth [13]. Some nanodisks are observed to be partly overlapping, which likely creates pathways for effect charge transfer during the electrocatalytic reactions. On the other hand, Co_3O_4 nanoparticles exhibit non-uniform morphologies with a broad particle size distribution of 10 to 100 nm (Fig. 1b). Co_3O_4 nanodisks exhibit porosity on the two-dimensional surface (Fig. 1c), which likely enhances active site exposure and mass transport properties [12]. The TEM characterization also confirms two-dimensional nanodisk morphology with surface porosity (Fig. 1d), and the SAED analysis reveals a pattern that corresponds to spinel crystal structure (Fig. 1d, inset) [14]. In fact, the observed fringes correspond to the (111) d -spacing ($d = 0.46\text{ nm}$) of spinel Co_3O_4 (Fig. 1e) [14]. The FFT pattern is also characteristic of the (111) plane of spinel Co_3O_4 (Fig. 1e, inset) [14]. Lastly, XRD patterns show characteristic spinel oxide peaks for both nanodisks and nanoparticles (Fig. 1f) [8,14].

To emphasize the practicality of Co_3O_4 nanodisks in a real environment, all single-cell battery tests are performed utilizing air in ambient conditions instead of pressurized pure oxygen. The charge and discharge battery voltages of Co_3O_4 nanodisks obtained by the galvanodynamic testing clearly show significantly reduced over-potentials at all current densities measured compared to those of Co_3O_4 nanoparticles (Fig. 2a). Particularly at higher current densities, Co_3O_4 nanodisks significantly outperform the nanoparticles for both charge and discharge, consistent with the conjecture that the nanodisk

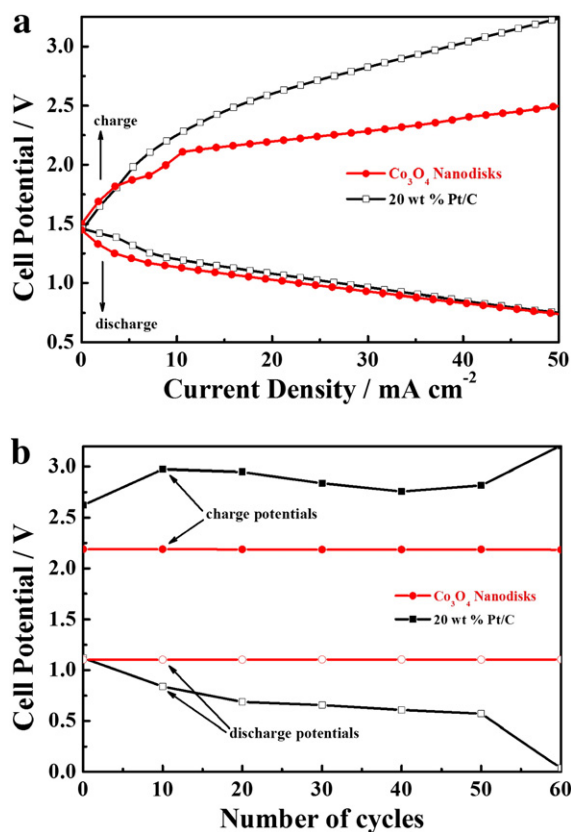


Fig. 3. (a) Galvanodynamic charge/discharge profiles, and (b) battery voltages obtained by galvanostatic pulse cycling of Co_3O_4 nanodisks (red) and commercial Pt/C (black).

morphology and partly overlapped interactions improve the charge transport properties which in turn mitigates observed overpotentials. In fact, the lower battery resistances of Co_3O_4 nanodisks are directly evaluated from the Nyquist plots by conducting EIS (Fig. 2b). The Nyquist plot of a single-cell battery modeled by an equivalent circuit with internal (R_s), solid-electrolyte interface (R_{int}), and charge transfer (R_{ct}) resistances (Fig. 2b, inset) [8,15] results in lower values for Co_3O_4 nanodisks compared those of the nanoparticles (Table 1). In particular, significantly lower R_{ct} is indicative of superior electrical properties during the electrocatalytic reaction over the two-dimensional porous surface. Furthermore, the rechargeability of Co_3O_4 nanodisks is evaluated by pulse cycling where virtually no voltage fading has been observed even after 60 cycles (Fig. 2c), whereas the nanoparticles have exhibited voltage losses for both charge and discharge of 3.9 and 11%, respectively (Fig. 2d). The excellent rechargeability of Co_3O_4 nanodisks is attributed to the reduced overpotentials particularly for the charge voltage, which significantly lessens the electrochemical degradation of the air cathode [16,17]. The high charge voltages observed with the nanoparticles, however, most likely have led to the carbon corrosion of GDL and oxidation of the catalyst [16,17]. These result in the loss of catalytically active surface area and deactivation of the catalyst, which negatively affect the battery voltages over the course of cycling.

The commercial viability of Co_3O_4 nanodisks as highly efficient electrocatalyst is apparent from comparable galvanodynamic discharge and much improved charge voltages compared to those of state-of-art

20 wt.% Pt/C catalyst (Fig. 3a). Furthermore, Co_3O_4 nanodisks demonstrate excellent rechargeability with negligible voltage fading, whereas Pt/C shows significant drops for both discharge and charge over 60 pulse cycles, likely due to the carbon degradation of GDL, and Pt dissolution and agglomeration (Fig. 3b) [17,18]. These results emphasize Co_3O_4 nanodisks as highly efficient and stable bi-functional catalyst facilitated by the reduced overpotentials, attributed to the morphological effect of enhanced mass diffusion and charge transfer.

4. Conclusion

Highly active and durable Co_3O_4 nanodisk catalyst with bi-functionality towards both the oxygen reduction and evolution reactions has been successfully synthesized for rechargeable zinc-air batteries utilizing ambient air. The galvanodynamic testing of Co_3O_4 nanodisks reveals superior charge and discharge voltages with excellent rechargeability demonstrated by 60 pulse cycles with no voltage fading. These advantages of Co_3O_4 nanodisks are attributed to the two-dimensional porous nanodisk morphology that facilitates mass diffusion and charge transport during electrocatalysis. This reduces the electrical resistances associated with the battery operation as confirmed by electrochemical impedance spectroscopy. Furthermore, the discharge performance of Co_3O_4 nanodisks is comparable to that of state-of-art Pt/C catalyst with much improved rechargeability demonstrated by pulse cycling, highlighting the practicality of Co_3O_4 nanodisks as efficient and stable bi-functional catalyst for rechargeable zinc-air battery applications.

5. Conflict of interest

The authors state that there is no conflict of interest.

Acknowledgment

This work was financially supported by the Natural Sciences and Engineering Research Council of Canada (NSERC Idea to Innovation Grants I2IPJ 445388-13) and the University of Waterloo.

References

- [1] J.-S. Lee, S. Tai Kim, R. Cao, N.-S. Choi, M. Liu, K.T. Lee, J. Cho, *Adv. Energy Mater.* 1 (2011) 34.
- [2] Z. Chen, A. Yu, D. Higgins, H. Li, H. Wang, Z. Chen, *Nano Lett.* 12 (2012) 1946.
- [3] M. Prabu, P. Ramakrishnan, S. Shanmugam, *Electrochem. Commun.* 41 (2014) 59.
- [4] M. Prabu, K. Ketpang, S. Shanmugam, *Nanoscale* 6 (2014) 3173.
- [5] Z.-L. Wang, D. Xu, J.-J. Xu, X.-B. Zhang, *Chem. Soc. Rev.* (2014), <http://dx.doi.org/10.1039/C3CS60248F>.
- [6] M.A. Rahman, X. Wang, C. Wen, *J. Electrochem. Soc.* 160 (2013) A1759.
- [7] V. Neburchilov, H.J. Wang, J.J. Martin, W. Qu, *J. Power Sources* 195 (2010) 1271.
- [8] D.U. Lee, J.-Y. Choi, K. Feng, H.W. Park, Z. Chen, *Adv. Energy Mater.* (2013), <http://dx.doi.org/10.1002/aenm.201301389>.
- [9] H.W. Park, D.U. Lee, Y. Liu, J. Wu, L.F. Nazar, Z. Chen, *J. Electrochem. Soc.* 160 (2013) A2244.
- [10] Z. Chen, M. Waje, W. Li, Y. Yan, *Angew. Chem.* 119 (2007) 4138.
- [11] T. Ioroi, N. Kitazawa, K. Yasuda, Y. Yamamoto, H. Takenaka, *J. Electrochem. Soc.* 147 (2000) 2018.
- [12] D.U. Lee, B.J. Kim, Z. Chen, *J. Mater. Chem.* 1 (2013) 4754.
- [13] Y. Sun, Y. Xia, *Science* 298 (2002) 2176.
- [14] Y. Hou, H. Kondoh, M. Shimojo, T. Kogure, T. Ohta, *J. Phys. Chem. B* 109 (2005) 19094.
- [15] D. Thiele, A. Züttel, *J. Power Sources* 183 (2008) 590.
- [16] L.M. Roen, C.H. Paik, T.D. Jarvi, *Electrochem. Solid-State Lett.* 7 (2004) A19.
- [17] X. Wang, W. Li, Z. Chen, M. Waje, Y. Yan, *J. Power Sources* 158 (2006) 154.
- [18] J. Zhang, K. Sasaki, E. Sutter, R.R. Adzic, *Science* 315 (2007) 220.